Neuroscience 157 (2008) 577–587

A NOVEL *KCNA1* MUTATION IDENTIFIED IN AN ITALIAN FAMILY AFFECTED BY EPISODIC ATAXIA TYPE 1

P. IMBRICI,[e1] F. GUALANDI,[a1] M. C. D'ADAMO,[e] M. TADDEI MASIERI,[a] P. CUDIA,[b] D. DE GRANDIS,[b] R. MANNUCCI,[c] I. NICOLETTI,[c] S. J. TUCKER,[d] A. FERLINI[a] AND M. PESSIA[e]*

[a]*Section of Medical Genetics, University of Ferrara, Italy*

[b]*Department of Neuroscience, Hospital of Rovigo, Italy*

[c]*Section of Internal Medicine and Oncology, Department of Clinical and Experimental Medicine, University of Perugia, School of Medicine, Perugia, Italy*

[d]*Department of Physics, Clarendon Laboratory, University of Oxford, Oxford, UK*

[e]*Section of Human Physiology, Department of Internal Medicine, University of Perugia School of Medicine, Via del Giochetto, I-06126 Perugia, Italy*

Abstract—Episodic ataxia type 1 (EA1) is a rare human neurological syndrome characterized by continuous myokymia and attacks of generalized ataxia that can be triggered by abrupt movements, emotional stress and fatigue. An Italian family has been identified where related members displayed continuous myokymia, episodes of ataxia, attacks characterized by myokymia only, and neuromyotonia. A novel missense mutation (F414C), in the C-terminal region of the K^+ channel Kv1.1, was identified in the affected individuals. The mutant homotetrameric channels were non-functional in *Xenopus laevis* oocytes. In addition, heteromeric channels resulting from the co-expression of wild-type Kv1.1 and Kv1.1(F414C), or wild-type Kv1.2 and Kv1.1(F414C) subunits displayed reduced current amplitudes and altered gating properties. This indicates that the pathogenic effect of this *KCNA1* mutation is likely to be related to the defective functional properties we have identified.

Key words: episodic ataxia, ion channel gene defects, Kv1.1, Kv1.2 cerebellum, *Xenopus* oocytes, confocal microscopy.

Episodic ataxia type 1 (EA1) is an autosomal dominant disorder characterized by myokymia and attacks of ataxic gait that may be brought on by fever, startle, emotional stress, and fatigue (Van Dyke et al., 1975). The first symptoms typically manifest during childhood and can persist throughout adult life. Since the description of the first EA1 kindred by Van Dyke et al. (1975), the phenotypic spectrum of the disorder has widened considerably and it is now apparent that phenotypic differences exist not only between different families, but also between individuals within the same family. Patients have been reported with unusual symptoms such as partial epilepsy, EA1 without myokymia, isolated neuromyotonia, neuromuscular findings including joint contractures, postural abnormalities, skeletal deformities and paroxysmal dyspnea (Scheffer et al., 1998; Klein et al., 2004; Kinali et al., 2004; Shook et al., 2008). Some patients experience severe ataxia more than 15 times per day, whereas other individuals experience attacks less than once per month (Van Dyke et al., 1975). There is also heterogeneity in their response to treatment, with some kindreds being particularly resistant to drugs (Eunson et al., 2000).

Linkage studies in several EA1 families led to the discovery of a number of point mutations in the voltage-dependent potassium channel gene *KCNA1* (Kv1.1), on chromosome 12p13 (Browne et al., 1994, 1995; Comu et al., 1996; Litt et al., 1994; Eunson et al., 2000; Scheffer et al., 1998; Klein et al., 2004; Lee et al., 2004; Shook et al., 2008). The amino acid residues mutated in EA1 patients are at positions which are highly conserved in the delayed-rectifier potassium channel gene family, and functional studies have shown that these mutations generally impair Kv1.1 channel function, although with quite variable effects on channel assembly, trafficking and kinetics (Eunson et al., 2000; Adelman et al., 1995; Zerr et al., 1998; Zuberi et al., 1999; D'Adamo et al., 1998; Rea et al., 2002; Imbrici et al., 2003; Cusimano et al., 2004).

The voltage-gated potassium channel Kv1.1 shows significant cell-type and regional diversity in the nervous system where it forms both homomeric and heteromeric channels (e.g. with Kv1.2) and is extensively modulated by intracellular and extracellular factors. Recently, studies attempting to reproduce the *in vivo* condition have shown that EA1 mutations may also affect heteromeric Kv1 channel activity, thus widening the molecular consequences of the disease (D'Adamo et al., 1999; Rea et al., 2002; Maylie et al., 2002; Imbrici et al., 2007).

Despite several lines of evidence which indicate that defective delayed-rectifier K^+ channels cause cerebellar dysfunction, the molecular and neurological mechanisms of EA1 are still not completely understood (Kullmann et al., 2001; Rajakulendran et al., 2007). Here we report a Sicilian family displaying typical and atypical EA1 symptoms. Furthermore, by haplotype sharing and mutation analysis we have identified a new *KCNA1* mutation in the affected members that causes a complete *loss-of-function* of homotetrameric channels, and markedly reduced heteromeric current amplitudes as well as producing important changes in their intrinsic biophysical properties.

[1] These authors contributed equally to this work.

*Corresponding author. Tel: +39-075-5857375; fax: +39-075-5857371.
E-mail address: pessia@unipg.it (M. Pessia).

Abbreviations: AP, action potentials; d.o.b., date of birth; EA1, episodic ataxia type 1; GFP, green fluorescent protein; PCR, polymerase chain reaction; SNP, single nucleotide polymorphism; STR, short tandem repeats; TEVC, two-electrode voltage-clamp; VNTRs, variable number of tandem repeats; WT, wild-type.

0306-4522/08 © 2008 IBRO. Published by Elsevier Ltd. All rights reserved.
doi:10.1016/j.neuroscience.2008.09.022

EXPERIMENTAL PROCEDURES

Neurophysiology

Nerve conduction studies were performed using surface stimulating and recording electrodes. Median and ulnar motor action potentials (AP) were recorded bilaterally from the abductor pollicis brevis and the abductor digiti minimi muscles respectively, with stimulation at the wrist and elbow. Median and ulnar F wave latencies were recorded. Sural sensory nerve AP were recorded antidromically at the ankles following stimulation in the calf. Electromyography was performed with a concentric needle electrode from the biceps brachii and opponens pollicis muscles. Local ischemia was applied by inflation of a blood pressure cuff around the upper arm to 220 mm Hg for 3 min.

The experiments were undertaken with the understanding and written consent of each subject, with the approval of the appropriate local ethics committee, and in compliance with national legislation and the Code of Ethical Principles for Medical Research Involving Human Subjects of the World Medical Association (Declaration of Helsinki).

Genetics, molecular biology, oocyte preparation and RNA injection

Total genomic DNA was isolated from peripheral blood leukocytes by BIOROBOT (Qiagen, Hilden, Germany) and analyzed as detailed in Fig. 1. The coding sequence of the intronless *KCNA1* gene was amplified from genomic DNA by polymerase chain reaction (PCR) in five amplicons overlapping by at least 130 nucleotides (Table 1S). PCR reactions were performed according to the manufacturer's protocols (Takara, Shiga, Japan). PCR products were purified and then sequenced by ABI Prism 3130 sequencer (Applied Biosystems, Toroed, Norway). Haplotype sharing analysis was performed by using VNTRs (variable number of tandem repeats) surrounding the *KCNA1* locus. Fluorescently-labeled PCR primers were used to amplify a set of six short tandem repeats (STR) loci belonging to chromosome 12p13 (D12S1608, D12S1694, D12S1050, D12S99, D12S374, D12S1728) which span a 15 Mb region in 12p, including the *KCNA1* locus. Primer sequences and STR mapping information are available at http://www.ncbi.nlm.nih.gov/genome/sts/. PCR conditions were as described above. All PCR products were analyzed on an ABI3130 automated sequencer. The allele size was determined using GeneScan and Genotyper software. Sequence analysis also revealed segregation of four known *KCNA1* synonymous changes such as single nucleotide polymorphysms (SNPs) rs1063289 (Arg-Arg), rs1048500 (Cys-Cys), rs22279120 (Thr-Thr) and rs4766309 (Thr-Thr) those are available at http://www.ncbi.nlm.nih.gov/projects/SNP/. Analysis of 200 control chromosomes failed to identify TTC>TGC mutation at nt 1241.

The EA1 mutation (F414C) was introduced into the human Kv1.1 cDNA in the pBF oocyte expression vector by site-directed mutagenesis. Wild-type (WT) and mutant Kv1.1 constructs were also tagged with green fluorescent protein (GFP) at the C-terminus by removing the stop codon and fusing them in frame with GFP excised from the pEGFP-C1 vector (Clontech). Capped cRNAs were synthesized *in vitro*, as previously described (D'Adamo et al., 1998).

Xenopus laevis were deeply anesthetized with an aerated solution containing 3-aminobenzoic acid ethyl ester methansulfonate salt (5 mM) and sodium bicarbonate (60 mM), pH=7.3. To further reduce their suffering, *Xenopus laevis* underwent no more than two surgeries, separated by at least 3 weeks. Stages V–VI *Xenopus* oocytes were isolated, injected with 50 nl cRNAs and stored at 16 °C in fresh ND96 medium containing (mM): NaCl 96, KCl 2, $MgCl_2$ 1, $CaCl_2$ 1.8, Hepes 5, gentamicin 50 μg/ml (Sigma, Italy). Procedures involving *Xenopus laevis* and their care were in accordance with the regulations of the Italian Animal Welfare Act and were approved by the local Authority Veterinary Service, and

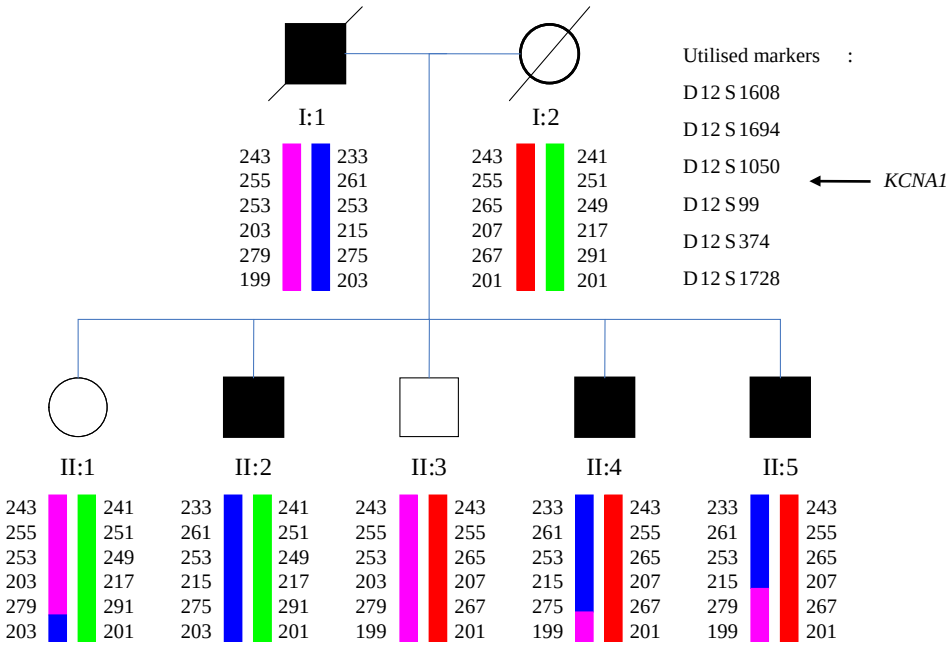

Fig. 1. Haplotype sharing of 12p13 region. The 12p13 haplotype shared by the four affected subjects (I:1, II:2, II:4, II:5) is depicted by a blue bar. *KCNA1* locus lies between D12S1050 and D12S99 markers. The utilized STRs spanning 15 MB region around the *KCNA1* locus (lying between D12S1050 and D12S99) are ordered according to their position in 12p from telomere to centromere. Six VNTRs were informative. Only the four affected males shared an identical haplotype in the region D12S1608-D12S99, which includes the *KCNA1* locus. Two recombination events between paternal chromosomes occurred in affected subjects, both without phenotypic effect being distal to the *KCNA1* locus. A recombination event between D12S374 and D12S1728 also occurred in a nonaffected II:1 female, preserving the WT *KCNA1* locus in the inherited paternal chromosome.

were in accordance with the NIH Guide for the Care and Use of Laboratory Animals. The minimal number of animals was used.

Electrophysiology

Two-electrode voltage-clamp (TEVC) recordings were performed from oocytes at ~22 °C and 1–8 days after injection (D'Adamo et al., 1998). A GeneClamp 500 amplifier (Axon Instruments, Foster City, CA, USA) interfaced to a PC computer with an ITC-16 interface (Instrutech Corporation, Longmont, CO, USA). Microelectrodes were filled with KCl 3 M and had resistances of 0.1–0.5 MΩ. The extracellular solution contained (mM): NaCl 96, KCl 2, $MgCl_2$ 1, $CaCl_2$ 1.8, Hepes 5, pH=7.4. Recordings were filtered at 2 kHz and acquired at 5 kHz with Pulse software and analyzed with either PulseFit (HEKA, Germany) or IGOR (WaveMetrics, Lake Oswego, OR, USA). Leak and capacitative currents were subtracted using a P/4 protocol.

Confocal microscopy

Confocal microscopy analysis of *Xenopus* oocytes, injected with GFP-tagged constructs, was performed on a Zeiss LSM 510 laser scanning confocal microscope (Jena, Germany) using a 10× objective. GFP fluorescence was excited with a 488-nm argon laser beam. Emissions were collected using a 515-565-nm band-pass filter. All images were acquired with the same experimental settings (laser power, pinhole diameter and PMT gain) and Image J was used for the quantification of fluorescence emission of the pixels corresponding to the oocyte's membrane. Three-dimensional re-construction of representative images was performed with the Surpass module of Imaris software (Bitplane, Zurich, Switzerland).

RESULTS

Case report

Case II:5. The proband (date of birth, d.o.b., 1974) was born to unrelated parents after a normal full-term pregnancy. He had normal motor development, but since an accidental shoulder injury at the age of 26, developed symptoms of intermittent cerebellar ataxia with sudden onset gait unsteadiness, slurred speech and leg rigidity during attacks; consciousness remained unaltered and there was no vertigo, nausea, diplopia, tinnitus or headache; cognition was also normal. Generally, the attacks lasted from seconds to a few minutes and occurred four to five times a month. They could occur without precipitation, but happened most frequently during fever, exertion, stress or startle. Treatment with acetazolamide 500 mg/day and oxcarbamazepine 900 mg/day was ineffective. Clonazepam 0.8 mg/day produced partial improvement. However, during a period of severe stress (both parents died in 2004) the frequency of attacks increased. Since then, the patient reported daily attacks of ataxia as well as episodes (lasting 5–10 min) of intense myokymia of the hand muscles without other neurological deficits and episodes of intense interictal neuromyotonia.

Since no reduction in attack severity occurred during clonazepam treatment, the drug was discontinued. Neurological examination, performed between attacks, revealed continuous myokymia in the small hand muscles and a tendency to keep his right fist clenched. Interictal deambulation did not reveal pathological features. Eye movements and coordination were normal. Nystagmus was absent. Full blood count, erythrocyte sedimentation rate, blood urea and electrolytes and thyroid function tests were normal.

Neurophysiological tests revealed resting electromyographic activity in the small hand and proximal upper limbs muscles. Spontaneous myokymic activity consisted of rhythmically repeated motor unit discharges with a frequency of $4 \cdot s^{-1}$ (Fig. 1S). The amplitude of the spontaneously occurring potentials was of the same amplitude as the motor unit potentials. The duration of the bursts was proportional to the number of spikes and ranged from 10 ms to 25 ms. The shape of the separate spikes was usually biphasic or polyphasic. During ischemia the myokymic discharges showed a gradual rise in frequency. The i.v. administration of 1 g of ionized calcium produced no significant variation of resting activity. F wave latency of median and ulnar nerves could not be detected because of the presence of continuous myokymic activity after the M response which disrupts the silent period necessary to visualize these waves. Motor and sensory nerve conduction velocities and distal motor latencies were normal. Cortical magnetic stimulation revealed that the central time motor conduction was normal. Moreover, somatosensory evoked potentials were within normal limits. Muscle and sural nerve biopsies performed prior to hospitalization were normal.

Case I:1. The proband's deceased father was reported to have finger myokymia and an occasional episode of gait unsteadiness precipitated by a stressful event.

Cases II:2 and II:4. The proband's two older brothers (d.o.b., 1966 and 1971, respectively) both had symptoms of intermittent ataxia and dysarthria since the age of 25. The attacks, precipitated only by fever or abrupt postural changes, were rare and very brief. For this reason none of them required medical treatment. Neurological interictal examination was unremarkable, except for mild finger myokymia.

Case III:7. The proband's nephew (d.o.b., 1994) developed attacks of ataxia at the age of 18–24 months when he first started walking. Currently the episodes, also characterized by dysarthria, are very rare and precipitated only by fever or profound physical efforts. The patient, at age 8, presented an isolated photosensitive generalized tonic–clonic seizure, which was not treated with anti epileptic drugs. He is still not under medication related to this condition.

Genetic analysis and expression pattern of F414C channels

Haplotype sharing analysis revealed that only the four affected males had an identical haplotype in common in the region D12S1608-D12S99, which includes the *KCNA1* locus (Fig. 1). By mutation analysis a novel heterozygous genetic defect was identified in all affected patients that changed nucleotide 1241 in the coding region from T>G. This mutation results in a highly conserved phenylalanine at position 414 at the end of the S6 transmembrane domain being changed into a cysteine (Fig. 2). Interestingly, this region is important for the control of gating in potassium channels. We therefore investigated the functional

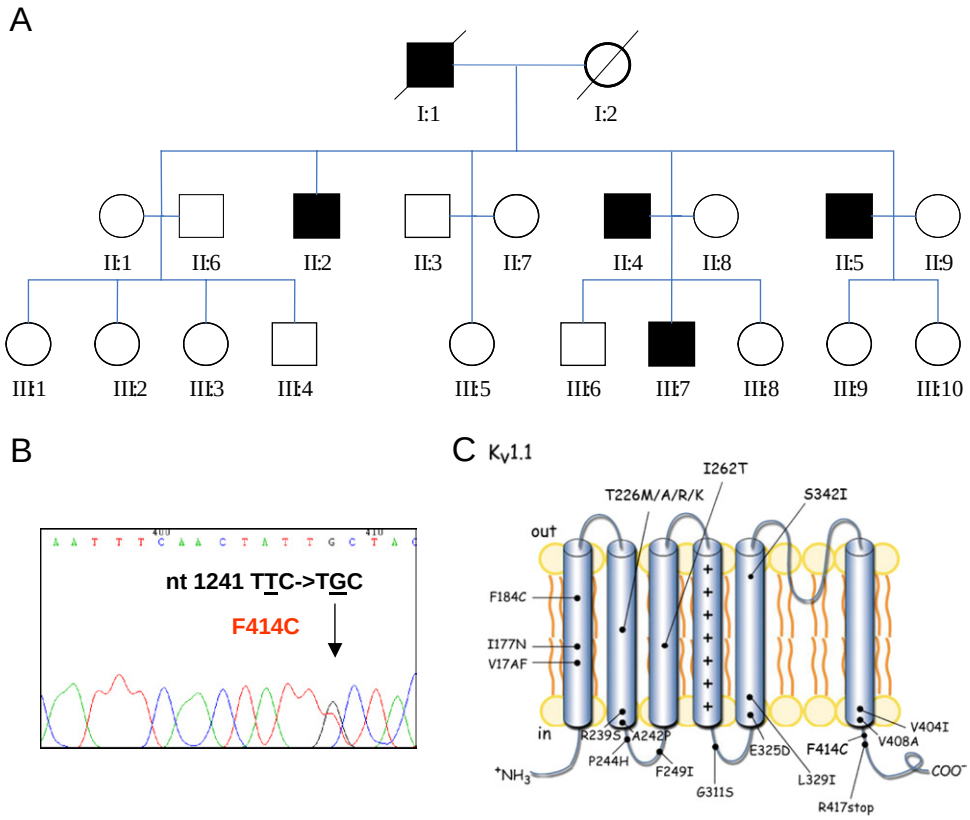

Fig. 2. Pedigree of the EA1 family and sequence analysis of the *KCNA1* coding region. (A) Schematic drawing of the three-generation family from Sicily affected by EA1. All affected patients harbor the novel mutation F414C in the *KCNA1* gene. (B) Sequence chromatogram of genomic DNA from a representative patient shows a double peak (arrow) at nucleotide 1241 that changes T>G, resulting in F414C mutation. This novel missense F414C mutation co-segregates with the pathological phenotype. Sequencing of the full *KCNA1* coding region was performed in subjects I:1, I:2, II:1, II:2, II:3, II:4, II:5 and III:7 of the EA1 family for mutation detection. This analysis allowed us to identify an heterozygous T>G transition at nucleotide 2346 in NM_000217 (nucleotide 1241 from *KCNA1* translation start codon), leading to a Phe to Cys substitution at codon 414 in the C-terminal region of the Kv1.1 subunit. (C) Conventional membrane topology of a human Kv1.1 subunit. The position of the mutations that have been identified in EA1 patients, including the F414C, is indicated. Four of such subunits are assembled to form a functional homotetrameric channel. Different subunits, belonging to Kv1 subfamily, may form heterotetrameric channels.

consequences of this F414C mutation on Kv1.1 function; F414C cRNA was *in vitro* transcribed and injected into oocytes and whole-cell currents recorded under TEVC configuration. However, no detectable currents were elicited by membrane depolarizations up to 170 mV, lasting up to 300 ms, from >100 oocytes injected with F414C cRNA, even at higher cRNA concentrations (~twofold increase; Fig. 3). By contrast, WT Kv1.1 cRNA injection gave rise to typical delayed-rectifier K^+ currents (Fig. 3; c.f. Fig. 1 in D'Adamo et al., 1998).

However, EA1 is an autosomal dominant disorder and the patients, harboring the F414C mutation, are heterozygous. Therefore, heteromeric channels composed of a mixture of WT and mutant subunits might be formed if both normal and mutated alleles are coexpressed. To address this issue, coexpression studies were carried out; equal amounts of WT and mutant RNAs were coinjected in the same oocyte and the results compared with those obtained from cells injected with an equivalent amount of WT RNA. The co-injection of WT and F414C cRNAs (1:1 ratio) resulted in an average current amplitude, at +60 mV, that was ~1.7-fold smaller than the control WT current (Fig. 3B). Moreover, ~twofold and ~fivefold F414C cRNA overexpression resulted in ~5.7-fold, ~12-fold WT current reduction, respectively (Fig. 3B; 1:2, 1:5 ratios).

These results indicate that F414C homotetrameric channel is nonfunctional, suggesting that the mutated Kv1.1 subunit may be recognized as an anomalous protein and degraded by the trafficking machinery of the cell before reaching the plasma membrane. Alternatively, the channel protein may be delivered normally to the plasma membrane, but could have a 'gating' defect and therefore be unable to open correctly. In order to discriminate between these possibilities we examined the expression pattern of F414C channels in *Xenopus laevis* oocytes, by analyzing the fluorescence intensity of cells injected with Kv1.1-GFP or Kv1.1(F414C)-GFP RNAs. Imaging studies with confocal microscopy suggest that the Kv1.1(F414C)-GFP construct displays an expression pattern similar to Kv1.1-GFP (Fig. 4). Furthermore, the biophysical properties of these GFP-tagged constructs were identical to the corresponding untagged channels (not shown). However, future studies using a combination of biochemical assays and confocal microscopy analysis of mammalian cells ex-

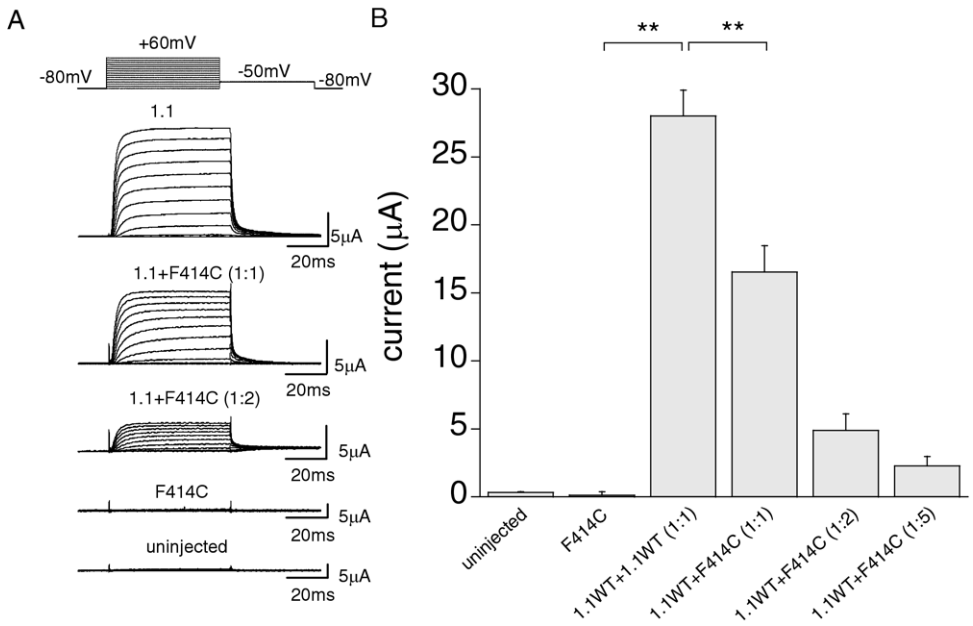

Fig. 3. The F414C mutation results in a nonfunctional homomeric channel and reduces WT current amplitude. (A) Sample current families recorded from oocytes expressing the indicated channels. The pulse protocol is indicated on top. Outward currents were evoked by 60 ms depolarizing commands from a holding potential of −80 mV. Notice that F414C expression resulted in whole-cell currents similar to uninjected oocytes. (B) Bar graph showing the average whole-cell current recorded at +60 mV from oocytes uninjected, injected with either Kv1.1(F414C) cRNA (F414C), WT cRNA (1.1WT+1.1WT) or co-injected with Kv1.1WT+Kv1.1(F414C) cRNAs (1.1WT+F414C; 1:1 ratio). The effects of F414C over-expression on WT currents were evaluated by increasing the amount of mutant cRNA co-injected with a constant amount of WT cRNA (1:2, 1:5 ratio). The overall procedure resulted in a progressive reduction in WT current amplitudes. Similar results were obtained from several independent experiments carried out at 24, 48 and 72 h after cRNA injection, by using different batches of oocytes (*not shown*). Data are mean±S.E.M. of 20–50 cells. The statistical significance was determined by using an unpaired Student's *t*-test. ** *P* values <0.001.

pressing these constructs are required to determine the precise levels of expression in the plasma membrane.

Functional characterization of heteromeric channels composed of WT Kv1.1 and Kv1.1(F414C) subunits

The functional analysis of heteromeric Kv1.1/Kv1.1(F414C) channels showed that their activation time constants were slightly slower and deactivation time constants slightly faster than WT channels (Fig. 5A; Table 1). Moreover, the current–voltage relationships revealed that these channels possess an average midpoint activation voltage ($V_{1/2}$) and slope factor (k) similar to WT channels (Fig. 5B; Table 1). WT Kv1.1 channels are characterized by a slow process of inactivation named C-type inactivation that increases progressively during intense neuronal activity, modifying both the firing rate and the shape of the APs (Aldrich et al., 1979). Thus, possible modifications of this distinct channel property may be pathophysiologically relevant for EA1. Indeed, the time course of current decay for heteromeric Kv1.1/Kv1.1(F414C) channels, determined by calculating the time constants, was much faster than for WT Kv1.1 (Fig. 5C; Table 1). This effect was more pronounced when a constant amount of WT cRNA was coinjected with a higher amount of F414C cRNA (1:2 ratio; Fig. 5C). Furthermore, heteromeric Kv1.1/Kv1.1(F414C) channels recovered from C-type inactivation with a time course significantly faster than for WT Kv1.1 (Fig. 5D; Table 1). This recovery was even faster when WT and Kv1.1(F414C) RNAs were co-injected at 1:2 ratio (Fig. 5D). Taken together these results show that the F414C mutation: *i*) causes a complete *loss-of-function* of Kv1.1(F414C) homotetramers; *ii*) markedly reduces WT current amplitudes and *iii*) accelerates C-type inactivation and shortens the refractory period of heteromeric Kv1.1/Kv1.1(F414C) channels.

Functional characterization of heteromeric channels composed of WT Kv1.2 and Kv1.1(F414C) subunits

Kv1.1 and Kv1.2 form heteromeric channels at the presynaptic terminals of cerebellar basket cells (Wang et al., 1993; Southan and Robertson, 1998). Alteration of the functional properties of cerebellar basket cell-Purkinje cell synapses may contribute to the cerebellar symptoms of EA1, such as ataxia and tremors (Herson et al., 2003). We therefore determined the effects of the F414C mutation on heteromeric Kv1.1/Kv1.2 channel function, as it would be of particular interest to EA1 pathophysiology.

Kv1.2/Kv1.1(F414C) cRNA co-expression, at 1:1, 1:2 and 1:5 ratios, resulted in progressively smaller current amplitudes (Fig. 6A and B). Moreover, the plot of the activation and deactivation time constants, as a function of membrane potentials, showed that the F414C mutation accelerated both opening and closing channel kinetics (Fig. 7A). In particular, the deactivation time constants of Kv1.2/Kv1.1(F414C) were ~2.2- and ~threefold faster at 1:1 and 1:2 co-injection ratios, respectively, compared with

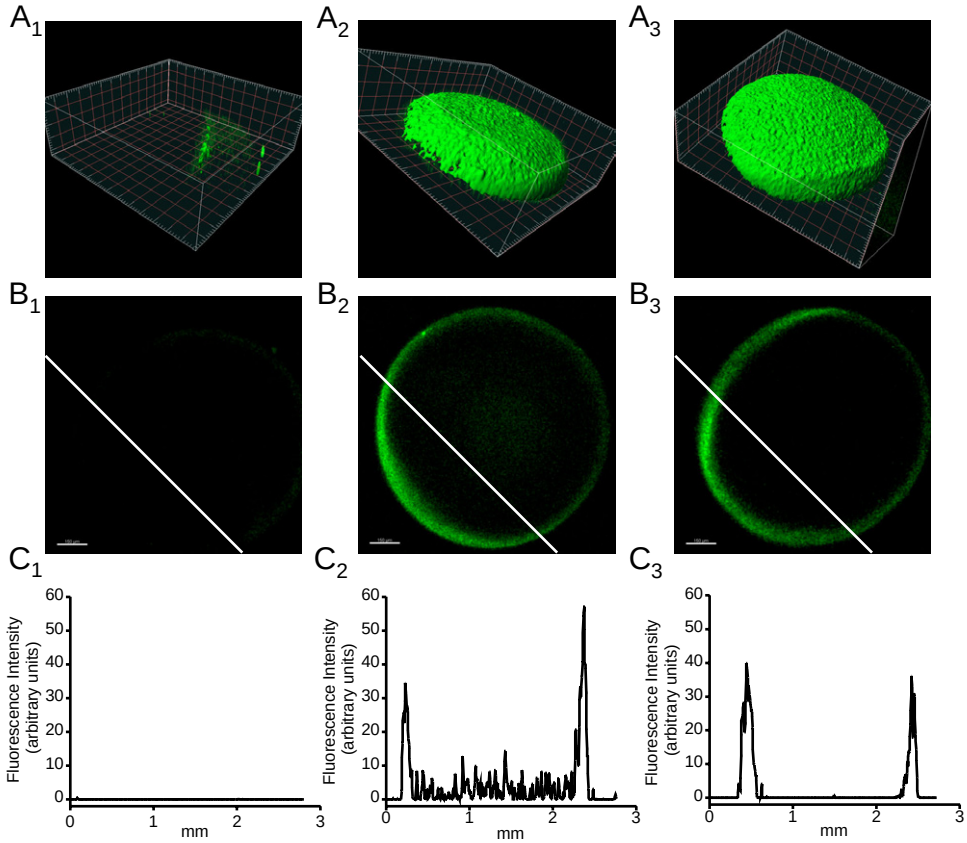

Fig. 4. Confocal microscopy analysis of Kv1.1(F414C) channels expression in *Xenopus laevis* oocytes. (A) 3D Reconstruction of the fluorescence surface profile of a representative uninjected oocyte (A_1) and of those injected with Kv1.1WT (A_2) and F414C (A_3) RNAs. (B_{1-3}) Fluorescence intensity, acquired at the equator, of the corresponding oocytes shown on top. Note that the Kv1.1(F414C)-GFP construct showed an expression pattern similar to Kv1.1WT, whereas, the fluorescence intensity of uninjected oocytes was almost absent. (C_{1-3}) Fluorescence intensity plots of line profile analysis of corresponding images in B_{1-3}.

Kv1.2/Kv1.1WT (Fig. 7A; *see inset for direct comparison*; Table 2). Another pronounced effect of the F414C mutation was an approximately 18 mV right-shift of the midpoint activation voltage ($V_{1/2}$) of heteromeric channels compared with WT (Fig. 7B; Table 2). By contrast, the $V_{1/2}$ of the heteromeric Kv1.1/Kv1.1(F414C) channels, was right-shifted by only 2–3 mV compared with WT (Table 1). Both, the time course of C-type inactivation and recovery from inactivation, for the mutated heteromeric channels, were faster than WT Kv1.1 and increased with the amount of mutant cRNA injected (Fig. 7C and D; Table 2). In summary, these results show that the F414C mutation also impairs heteromeric Kv1.1/Kv1.2 channel function by: *i*) reducing WT current amplitudes; *ii*) markedly speeding up the deactivation kinetics of the channel; *iii*) shifting the current–voltage relationships to more depolarized potentials; and *iv*) accelerating C-type inactivation, which further reduces channel availability and shortens the refractory period of these channels.

DISCUSSION

Here, we have described a Sicilian family affected by EA1 that is characterized by typical and atypical clinical symptoms (Van Dyke et al., 1975; Brunt and van Weerden, 1990; Eunson et al., 2000). A large degree of variability in the onset of the disease, frequency of the attacks, clinical symptoms and high drug resistance were reported by family members, as has been described for many other EA1-affected patients (Rajakulendran et al., 2007). Interictal neuromyotonia, leg rigidity during attacks (neuromyotonia), episodes of intense myokymic activity during attacks without ataxia and other neurological deficits are less commonly observed among the EA1 patients described so far. Indeed, clinical symptoms such as distal weakness, prolonged neuromyotonia and stiffness with inability to walk have been described in only a few cases (Gancher and Nutt, 1986; Brunt and van Weerden, 1990; Eunson et al., 2000; Klein et al., 2004). Furthermore, the proband shows a very specific phenotype, characterized by increasing frequency of attacks with ageing, as well as a relationship between both the onset and the worsening of the disease with a specific traumatic physical or emotional event. The isolated photosensitive generalized tonic–clonic seizure reported by the proband's nephew is not sufficient to make a diagnosis of epilepsy, although the involvement of the new genetic defect cannot be excluded.

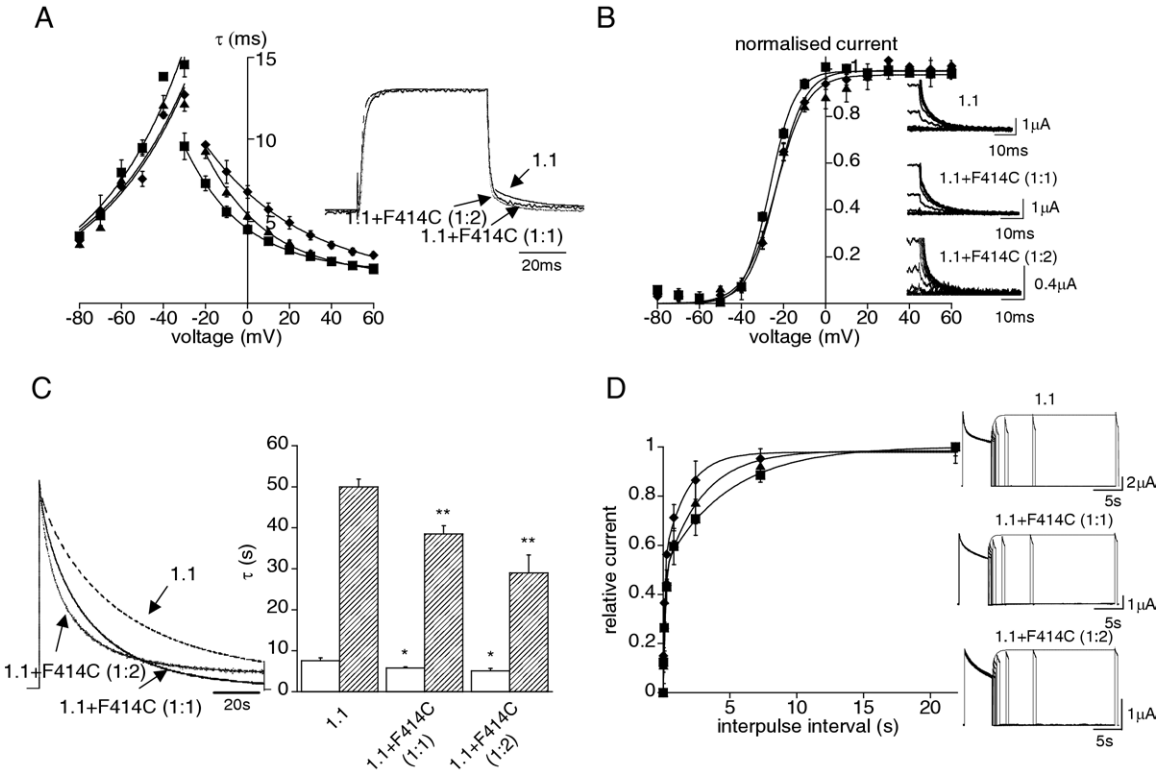

Fig. 5. The F414C mutation speeds up the C-type inactivation and recovery from inactivation of heteromeric Kv1.1/Kv1.1(F414C) channels. (A) The activating and deactivating current traces were fitted with a single exponential function, in order to assess the effects of the F414C mutation on the activation and deactivation kinetics of the channel. The relevant time constants for the human Kv1.1 (■), Kv1.1+F414C (▲; 1:1 ratio) and Kv1.1+F414C (♦; 1:2 ratio) channels were calculated and plotted as a function of the test pulse. The solid line shows the fit of the data points with the equation: $\tau=\tau_{V1/2}\exp\{(V-V_{1/2})/k\}$, where $\tau_{V1/2}$ is the time constant at the $V_{1/2}$ of the channels and k is the slope factor for the voltage dependence of the time constants. This plot shows that the mutation exerts little effect on the activation–deactivation of the channel which can be directly observed also from the representative current trace recorded at +60 mV for WT channels, overlain with that resulting from the co-injection of WT and F414C cRNAs (1:1 and 1:2 ratio; inset). (B) The voltage-dependence of channel activation for Kv1.1WT (■), Kv1.1+F414C (▲; 1:1 ratio) and Kv1.1+F414C (♦; 1:2 ratio) was determined by recording tail currents at −50 mV, after prepulse commands to several voltages. The normalized current–voltage data points were fitted with the Boltzmann function $I=1/1+\exp\{-(V-V_{1/2})/k\}$ from which the $V_{1/2}$ and slope factor k were calculated. The inset, on the right hand side, shows representative tail current families for the indicated channels recorded at −50 mV. Notice that the mutation changes very little the voltage-dependence of heterozygous channels. (C) To determine the C-type inactivation kinetics, a test pulse to +60 mV for 3.5 min was delivered to oocytes expressing WT and heteromeric channels and the decaying phase of the current was fitted with a double-exponential function from which the time constants were calculated. The left panel shows the normalized current traces resulting from either the expression of Kv1.1 alone (dashed line) or from the co-expression of WT and F414C cRNA at 1:1 (solid line) and 1:2 (dotted line) ratios. The bar graph shows the fast (white bar) and slow (dashed bar) time constants of the C-type inactivation for the indicated channels. These results clearly show that the mutation speeds up the inactivation kinetics of heteromeric channels. (D) The recovery from C-type inactivation was determined by using a double-pulse protocol to +60 mV, separated by interpulse intervals of increasing duration (range: 0.010–21.87 s). The current amplitudes evoked by the second pulse (test) were divided by the first pulse (conditioning), normalized and plotted as a function of the interpulse interval. The solid curves indicate the fit of the data points with a double-exponential function from which the time constants were calculated for Kv1.1WT (■), Kv1.1+F414C (▲; 1:1) and Kv1.1+F414C (♦; 1:2). The inset shows sample current traces evoked by the two-pulse protocol for the indicated channels. The superimposed solid line shows the fit of the peak current, evoked by the test pulse, with a double-exponential function. Note that the mutation speeds up the recovery from inactivation. A careful evaluation of the biophysical properties of channels, resulting from injections at 1:5 ratio, was not possible due to marked current reduction. Data are means±S.E.M. of 10–15 cells. Student's *t*-test: * *P* values <0.05; ** *P* values <0.001.

However, genetic analysis of this family that included both a new linkage study and mutation screening, resulted in the identification of a novel mutation in the *KCNA1* potassium channel gene that results in the substitution of a highly conserved phenylalanine with a cysteine at position 414.

Although the Kv1.1(F414C) homotetrameric channels were nonfunctional, confocal imaging analysis of Kv1.1-GFP and Kv1.1(F414C)-GFP injected oocytes suggests that the mutated channels are delivered to the plasma membrane, at least in part, but unable to open correctly. By contrast, the R417X truncation mutant, which is located close to the F414C, results in a protein that is nonfunctional, but which is preferentially retained in the cytoplasm (Rea et al., 2002). However, the R417X truncation removes the C-terminus (and associated trafficking signals) and is therefore likely to result in a highly aberrant protein.

Even though co-expression with the Kv1.1(F4141C) mutant subunit resulted in a reduction in the current am-

Table 1. Biophysical parameters of Kv1.1WT and Kv1.1WT/Kv1.1F414C channels

Voltage	Voltage dependence of activation		Kinetic of activation, $\tau_{V1/2}$ (ms)	Kinetic of deactivation, $\tau_{V1/2}$ (ms)	C-type inactivation		Recovery from C-type inactivation	
	$V_{1/2}$ (mV)	k (mV)			τ_{fast} (s)	τ_{slow} (s)	τ_{fast} (ms)	τ_{slow} (s)
Kv1.1	−26.4±0.4	6.0±0.2	6.4±0.1	17.6±1.0	7.6±0.7 (22%)	50.0±1.9 (78%)	134±30 (50%)	4.8±1.4 (50%)
Kv1.1+Kv1.1F414C (1:1)	−23.8±0.4	7.3±0.2	8.6±0.2	15.3±1.5	5.8±0.3* (26%)	38.5±2.0** (74%)	102±23 (49%)	2.8±0.6 (51%)
Kv1.1+Kv1.1F414C (1:2)	−23.4±0.4	6.8±0.2	9.9±0.2	15.0±1.5	5.1±0.6* (38%)	29.0±4.4** (62%)	73±13* (56%)	1.7±0.3 (44%)

The data are the means±S.E.M. of 10–15 cells. The values in parentheses are the mean amplitudes of the fast and slow components, expressed as percentages.

* *P* values <0.05, Student's *t*-test.

** *P* values <0.001, Student's *t*-test.

plitudes of WT Kv1.1 and heteromeric Kv1.1/Kv1.2, this reduction was not enough to be considered a *dominant negative effect*. Another peculiarity of the F414C mutation is its ability to impair the biophysical properties of currents resulting from the co-expression of Kv1.1/Kv1.2 subunits more dramatically than those of WT Kv1.1 subunits. In fact, the activation–deactivation kinetics and the voltage-dependence of WT Kv1.1 channels were only slightly affected by the mutant F414C subunit. By contrast, the deactivation time constant of mutant heteromeric Kv1.1(F414C)/Kv1.2 currents was ~2.2-fold faster than their WT equivalent and the mutation right-shifted the $V_{1/2}$ by ~18 mV.

The overexpression study showed that the mutated subunit reduces current amplitudes and impairs their biophysical properties in a way that is dependent on the ratio of co-injected cRNAs. These results strongly suggest that the degree of impairment is related to the number of F414C subunits incorporated into the channels (D'Adamo et al., 1998), which strictly depends on the relative amounts of the different cRNAs co-injected (Kavanaugh et al., 1992; Rea et al., 2002). Possibly, individual variability in transcription and translation processing of the WT and mutated genes may generate channels with different stoichiometries and functional defects. Interestingly, this mechanism may account for the high degree of inter- and intrafamilial symptomatic variation.

The functionality of specific circuits within the CNS and PNS may also be impacted by these phenomena. It has been postulated that the attacks of cerebellar ataxia may

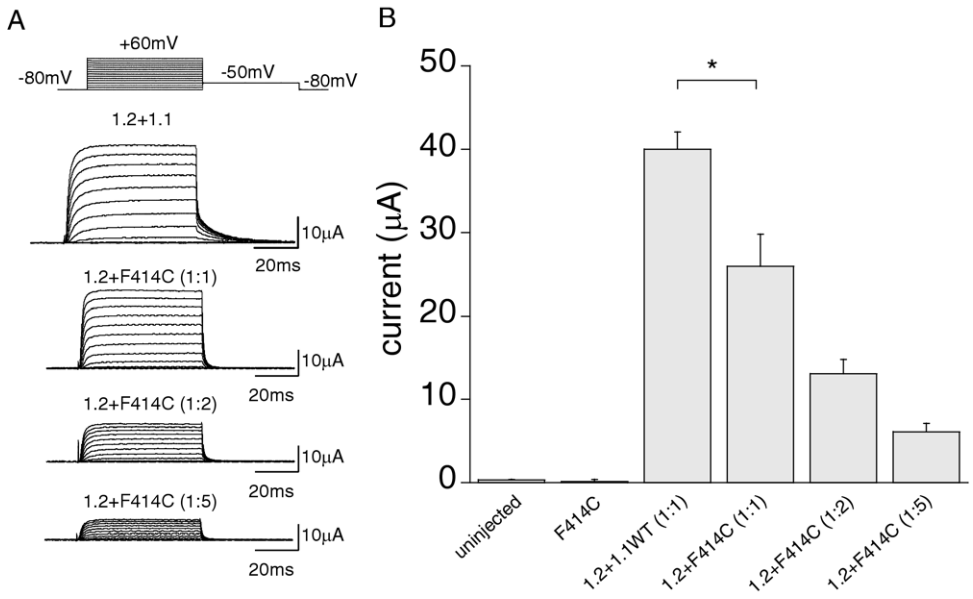

Fig. 6. The F414C mutation reduces the current amplitude of heteromeric channels composed of Kv1.2 and Kv1.1 subunits. (A) Sample families of current recorded from oocytes expressing the indicated channels. The pulse protocol is indicated on top. (B) Bar graph showing the average whole-cell current recorded from oocytes: uninjected, injected with Kv1.1(F414C) cRNA (F414C), with 1:1 ratio of Kv1.2 and Kv1.1WT cRNAs and with 1:1, 1:2 and 1:5 ratios of Kv1.2 to mutant cRNA. The currents were evoked by 60 ms depolarizing command at +60 mV, from a holding potential of −80 mV. Data are mean±S.E.M. of 6 to 10 cells. The statistical significance was determined by using an unpaired Student's *t*-test. * *P* values <0.05.

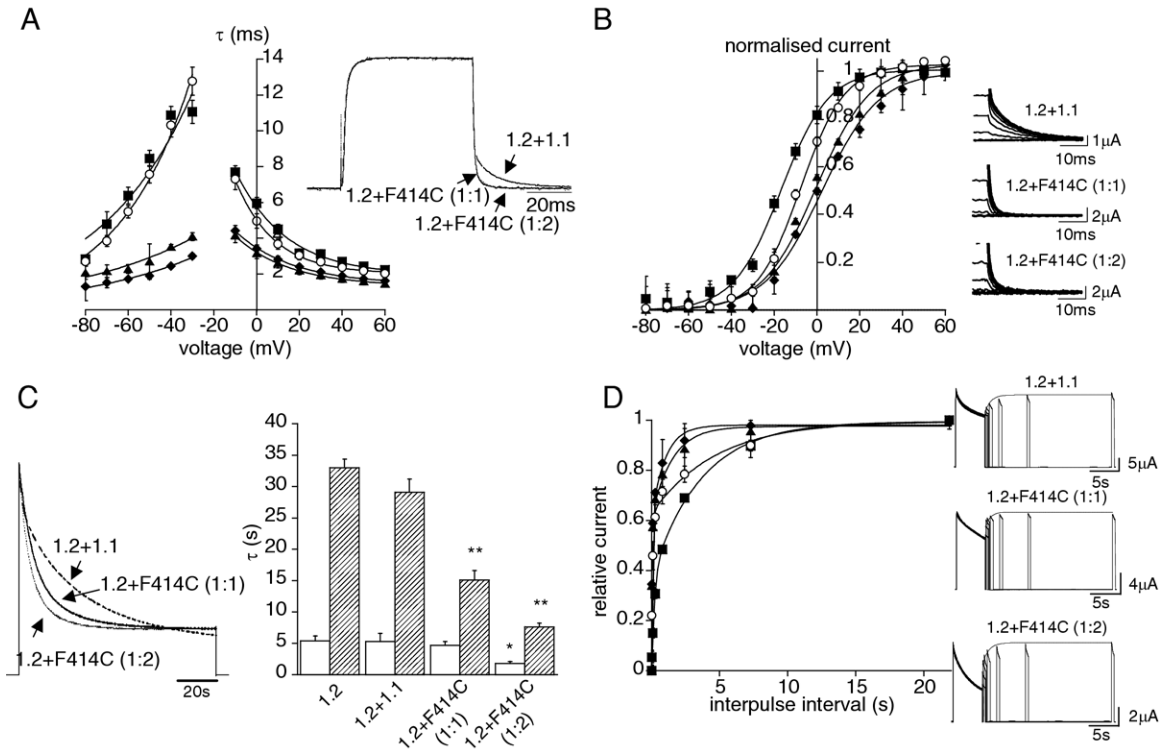

Fig. 7. The F414C mutation alters the kinetics of activation–deactivation, voltage-dependence and C-type inactivation in heteromeric Kv1.1/Kv1.2 channels. (A) Activating and deactivating current traces were recorded at different potentials and fitted with a single exponential function, in order to calculate the relative time constants for Kv1.2 (○), Kv1.2+Kv1.1 (■), Kv1.2+F414C (▲; 1:1 ratio) and Kv1.2+F414C (♦; 1:2 ratio) channels and plot them as a function of the test pulse. The data points were fitted as in Fig. 5A. The inset shows representative current traces recorded at +60 mV for Kv1.2+Kv1.1 channels normalized and overlain with those resulting from the co-injection of Kv1.2 with F414C cRNAs (1:1 and 1:2 ratio). Notice that the heteromeric channels carrying the mutation deactivate much faster than the WT. (B) Current–voltage relationships obtained by plotting the peak tail currents recorded at −50 mV as a function of the pre-pulse potential for Kv1.2 (○), Kv1.2+Kv1.1 (■), Kv1.2+F414C (▲; 1:1 ratio) and Kv1.2+F414C (♦; 1:2 ratio) channels. The solid curves indicate the fit of the data points with the Boltzmann function that is significantly right-shifted by the mutation. The inset, on the right hand side, shows representative tail current families recorded at −50 mV for the indicated channels. (C) Normalized current traces evoked by depolarizing steps at +60 mV, lasting 3.5 min, and delivered to oocytes co-expressing either Kv1.2+Kv1.1 (dashed line) or Kv1.2+F414C (1:1 and 1:2 ratio; solid and dotted lines, respectively; left panel). The currents resulting from the activation of the mutated channels decayed faster than the WT. Therefore, they were fitted with double-exponential functions to calculate the relevant time constants. The bar graph shows the fast (white bar) and slow (dashed bar) averaged time constants of the C-type inactivation, which were decreased by the mutation, concentration dependently. (D) Recovery from C-type inactivation for Kv1.2 (○), Kv1.2+Kv1.1 (■), Kv1.2+F414C (▲; 1:1 ratio) and Kv1.2+F414C (♦; 1:2 ratio) channels determined as detailed in Fig. 5D. The solid curves indicate the fit of the data points with a double-exponential function from which the time constants were calculated. The expression of the mutated subunit accelerates the recovery from inactivation, concentration dependently. The inset shows sample current traces evoked by the two-pulse protocol and then fit with a double exponential function (solid line). Data are means±S.E.M. of 10–15 cells. Student's *t*-test: * *P* values <0.05; ** *P* values <0.001.

result from altered GABAergic transmission at the basket cell–Purkinje cell synapse due to impaired Kv1.1/Kv1.2 channel function. Indeed, electrophysiological recordings from knock-in mice, harboring the EA1 mutation V408A

Table 2. Biophysical parameters of Kv1.2+Kv1.1WT and Kv1.2WT/Kv1.1F414C channels

Voltage	Voltage dependence of activation		Kinetic of activation, $\tau_{V1/2}$ (ms)	Kinetic of deactivation, $\tau_{V1/2}$ (ms)	C-type inactivation		Recovery from C-type inactivation	
	$V_{1/2}$ (mV)	k (mV)			τ_{fast} (s)	τ_{slow} (s)	τ_{fast} (ms)	τ_{slow} (s)
Kv1.2	−8.3±0.5	10.0±0.5	5.3±0.1	23.0±1.2	5.4±0.8 (23%)	33.0±1.4 (77%)	278±5 (54%)	1.5±0.2 (38%)
Kv1.2+Kv1.1	−18.3±0.5	12.0±0.5	3.3±0.1	15.0±1.7	5.3±1.3 (24%)	29.1±2.1 (76%)	311±86 (62%)	2.8±0.6 (38%)
Kv1.2+Kv1.1F414C (1:1)	−0.3±1.3**	12.5±1.1	1.7±0.06	6.7±0.7**	4.7±0.6 (51%)	15.1±1.5** (49%)	255±40 (71%)	2.4±0.3 (29%)
Kv1.2+Kv1.1F414C (1:2)	2.3±1.4**	13.0±1.1	2.1±0.05	4.9±0.3**	1.8±0.3* (23%)	7.6±0.6** (77%)	120±28* (71%)	1.8±0.3 (29%)

The data are the means±S.E.M. of 10–15 cells. The values in parentheses are the mean amplitudes of the fast and slow components, expressed as percentages.

* *P* values <0.05, Student's *t*-test.

** *P* values <0.001, Student's *t*-test.

(V408A/+), revealed an increased amplitude and frequency of GABAergic IPSCs onto cerebellar Purkinje cells, compared with WT animals (Herson et al., 2003). This evidence supports the hypothesis that an increased GABA release from presynaptic basket cells onto Purkinje cells may alter the output of the cerebellar cortex which provides the signals required for motor planning, execution and coordination (Ito, 1984). Likely, the gating defects caused by the F414C mutation on Kv1.1/Kv1.2 currents may alter the GABAergic inputs from cerebellar basket cells to Purkinje cells as reported for V408A/+ mice (Herson et al., 2003).

CONCLUSION

In conclusion, a novel F414C mutation has been identified in an Italian family displaying distinct phenotypic characteristics. Both homomeric and heteromeric Kv1 channel function is severely affected by this mutation, but although all affected patients harbor the same genetic defect, the intrafamilial symptoms are highly variable. The mechanisms accounting for such a phenotypic variability, its episodic nature, and how different stimuli trigger the attacks of ataxia and epilepsy are mostly unknown and remain a major challenge for future research into this and other neurological diseases.

Acknowledgments—The financial support of Telethon-Italy (grant no. GGP030159), of MIUR-COFIN 2005, of COMPAGNIA di San Paolo (Turin), the Fondazione Cassa di Risparmio di Perugia, and the Royal Society (London, UK) is gratefully acknowledged. Paola Imbrici is the recipient of a Ph.D. fellowship from COMPAGNIA di San Paolo (Turin). We thank Ezio Mezzasoma and Domenico Bambagioni for outstanding technical assistance and Andria D'Orazio for initial work. Finally, we would also like to express our gratitude to the Italian Red Cross (women's section of Perugia) for the donation of scientific equipment to the Section of Human Physiology for this research.

REFERENCES

Adelman JP, Bond CT, Pessia M, Maylie J (1995) Episodic ataxia results from voltage-dependent potassium channels with altered functions. Neuron 15:1449–1454.

Aldrich RW Jr, Getting PA, Thompson SH (1979) Inactivation of delayed outward current in molluscan neurone somata. J Physiol 291:507–530.

Browne DL, Gancher ST, Nutt JG, Brunt ER, Smith EA, Kramer P, Litt M (1994) Episodic ataxia/myokymia syndrome is associated with point mutations in the human potassium channel gene, KCNA1. Nat Genet 8:136–140.

Browne DL, Brunt ER, Griggs RC, Nutt JG, Gancher ST, Smith EA, Litt M (1995) Identification of two new KCNA1 mutations in episodic ataxia/myokymia families. Hum Mol Genet 4:1671–1672.

Brunt ERP, van Weerden TW (1990) Familial paroxysmal kinesigenic ataxia and continuous myokymia. Brain 113:1361–1382.

Comu S, Giuliani M, Narayanan V (1996) Episodic ataxia and myokymia syndrome: a new mutation of potassium channel gene Kv1.1. Ann Neurol 40:684–687.

Cusimano A, D'Adamo MC, Pessia M (2004) An episodic ataxia type-1 mutation in the S1 segment sensitises the hKv1.1 potassium channel to extracellular Zn^{2+}. FEBS Lett 576:237–244.

D'Adamo MC, Imbrici P, Sponcichetti F, Pessia M (1999) Mutations in the KCNA1 gene associated with episodic ataxia type-1 syndrome impair heteromeric voltage-gated K(+) channel function. FASEB J 13:1335–1345.

D'Adamo MC, Liu Z, Adelman JP, Maylie J, Pessia M (1998) Episodic ataxia type-1 mutations in the hKv1.1 cytoplasmic pore region alter the gating properties of the channel. EMBO J 17:1200–1207.

Eunson LH, Rea R, Zuberi SM, Youroukos S, Panayiotopoulos CP, Liguori R, Avoni P, McWilliam RC, Stephenson JB, Hanna MG, Kullmann DM, Spauschus A (2000) Clinical, genetic, and expression studies of mutations in the potassium channel gene KCNA1 reveal new phenotypic variability. Ann Neurol 48:647–656.

Gancher ST, Nutt JG (1986) Autosomal dominant episodic ataxia: a heterogeneous syndrome. Mov Disord 1:239–53.

Herson PS, Virk M, Rustay NR, Bond CT, Crabbe JC, Adelman JP, Maylie J (2003) A mouse model of episodic ataxia type-1. Nat Neurosci 6:378–383.

Imbrici P, Cusimano A, D'Adamo MC, De Curtis A, Pessia M (2003) Functional characterization of an episodic ataxia type-1 mutation occurring in the S1 segment of hKv1.1 channels. Pflugers Arch 446:373–379.

Imbrici P, D'Adamo MC, Cusimano A, Pessia M (2007) Episodic ataxia type 1 mutation F184C alters Zn^{2+}-induced modulation of the human K^+ channel Kv1.4-Kv1.1/Kvbeta1.1. Am J Physiol Cell Physiol 292:C778–C787.

Ito M (1984) The cerebellum and neural control. New York: Raven.

Kavanaugh MP, Hurst RS, Yakel J, Varnum MD, Adelman JP, North RA (1992) Multiple subunits of a voltage-dependent potassium channel contribute to the binding site for tetraethylammonium. Neuron 8:493–497.

Kinali M, Jungbluth H, Eunson LH, Sewry CA, Manzur AY, Mercuri E, Hanna MG, Muntoni F (2004) Expanding the phenotype of potassium channelopathy: severe neuromyotonia and skeletal deformities without prominent episodic ataxia. Neuromuscul Disord 14:689–693.

Klein A, Boltshauser E, Jen J, Baloh RW (2004) Episodic ataxia type 1 with distal weakness: a novel manifestation of a potassium channelopathy. Neuropediatrics 35:147–149.

Kullmann DM, Rea R, Spauschus A, Jouvenceau A (2001) The inherited episodic ataxias: how well do we understand the disease mechanisms? Neuroscientist 7:80–88.

Lee H, Wang H, Jen JC, Sabatti C, Baloh RW, Nelson SF (2004) A novel mutation in KCNA1 causes episodic ataxia without myokymia. Hum Mutat 24:536–542.

Litt M, Kramer P, Browne D, Gancher S, Brunt ER, Root D, Phromchotikul T, Dubay CJ, Nutt J (1994) A gene for episodic ataxia/myokymia maps to chromosome 12p13. Am J Hum Genet 55:702–709.

Maylie B, Bissonnette E, Virk M, Adelman JP, Maylie JG (2002) Episodic ataxia type 1 mutations in the human Kv1.1 potassium channel alter hKvbeta 1-induced N-type inactivation. J Neurosci 22:4786–4793.

Rajakulendran S, Schorge S, Kullmann DM, Hanna MG (2007) Episodic ataxia type 1: a neuronal potassium channelopathy. Neurotherapeutics 2:258–266.

Rea R, Spauschus A, Eunson L, Hanna MG, Kullmann DM (2002) Variable K^+ channel subunit dysfunction in inherited mutations of KCNA1. J Physiol 538:5–23.

Scheffer H, Brunt ER, Mol GJ, van der Vlies P, Stulp RP, Verlind E, Mantel G, Averyanov YN, Hofstra RM, Buys CH (1998) Three novel KCNA1 mutations in episodic ataxia type I families [published erratum appears in Hum Genet 1998, 102, 713]. Hum Genet 102:464–466.

Shook SJ, Mamsa H, Jen JC, Baloh RW, Zhou L (2008) Novel mutation in KCNA1 causes episodic ataxia with paroxysmal dyspnea. Muscle Nerve 37:399–402.

Southan AP, Robertson B (1998) Patch-clamp recordings form cerebellar basket cell bodies and their presynaptic terminals reveal an asymmetric distribution of voltage-gated potassium channels. J Neurosci 18:948–955.

Van Dyke DH, Griggs RC, Murphy MJ, Goldstein MN (1975) Hereditary myokymia and periodic ataxia. J Neurol Sci 25:109–118.
Wang H, Kunkel DD, Martin TM, Schwartzkroin PA, Tempel BL (1993) Heteromultimeric K^+ channels in terminal and juxtaparanodal regions of neurons. Nature 365:75–79.
Zerr P, Adelman JP, Maylie J (1998) Episodic ataxia mutations in Kv1.1 alter potassium channel function by dominant negative effects or haploinsufficiency. J Neurosci 18:2842–2848.
Zuberi SM, Eunson LH, Spauschus A, De Silva R, Tolmie J, Wood NW, McWilliam RC, Stephenson JP, Kullmann DM, Hanna MG (1999) A novel mutation in the human voltage-gated potassium channel gene (Kv1.1) associates with episodic ataxia type 1 and sometimes with partial epilepsy. Brain 122:817–825.

APPENDIX

Supplementary data

Supplementary data associated with this article can be found, in the online version, at doi:10.1016/j.neuroscience.2008.09.022.

(Accepted 11 September 2008)
(Available online 24 September 2008)